Journal of Hazardous Materials 175 (2010) 253–257

Contents lists available at ScienceDirect

Journal of Hazardous Materials

journal homepage: www.elsevier.com/locate/jhazmat

Kinetics determination of electrogenerated hydrogen peroxide (H_2O_2) using carbon fiber microelectrode in electroenzymatic degradation of phenolic compounds

Seung-Hee Cho [a], Am Jang [b], Paul L. Bishop [b], Seung-Hyeon Moon [c,*]

[a] Animal Environment Division, National Institute of Animal Science, Rural Development Administration, 77 Chuksan-gil, Kwonsun-Gu, Suwon 441-706, Republic of Korea
[b] Department of Civil and Environmental Engineering, University of Cincinnati, Cincinnati, OH 45221, USA
[c] Department of Environmental Science and Engineering, Gwangju Institute of Science and Technology (GIST), 261 Cheomdan-Gwagiro, Buk-gu, Gwangju 500-712, Republic of Korea

ARTICLE INFO

Article history:
Received 13 June 2009
Received in revised form
28 September 2009
Accepted 30 September 2009
Available online 6 October 2009

Keywords:
Carbon fiber microelectrode
Electrogeneration of hydrogen peroxide (H_2O_2)
Amperometry
Horseradish peroxidase (HRP)
Reticulated vitreous carbon (RVC)

ABSTRACT

The kinetics of electrogenerated hydrogen peroxide (H_2O_2), which can activate peroxidases in an electroenzymatic process, was examined by an amperometric technique using a carbon fiber microelectrode that was modified by polyaniline (PAn) film and platinum particles. The electrogeneration of H_2O_2 was found to be dependent on the pH and applied potential, and resulting in a variable current response of the carbon fiber microelectrode. The highest amount of H_2O_2 was electrogenerated when 2.3 V was applied between the Pt/Ti anode and a reticulated vitreous carbon (RVC) cathode at pH 6.0, with a current response of 0.0190 μA min^{-1}. Phenol was completely degraded by the electroenzymatic reaction of the immobilized horseradish peroxidase (HRP), and the time required for the electrogeneration of H_2O_2 increased according to the initial concentration of phenol. The degradation stoichiometric ratio between the electrogenerated H_2O_2 and the aqueous phenol under HRP immobilized on RVC was found to be 1:1.

1. Introduction

Hydrogen peroxide (H_2O_2) is widely used in many fields, especially the chemical industry and for environmental protection due to its strong oxidizing property and production of no hazardous residuals, degrading to only oxygen and water [1–8]. Also, it has been utilized in enzyme technologies as an activation compound for peroxidases such as lignin peroxide (LiP) and horseradish peroxidase (HRP). In the presence of H_2O_2 serving as an electron acceptor, LiP and HRP are activated and catalyze the oxidation of various organic substrates [9,10]. Therefore, it is clear that the catalytic reaction of peroxidase with H_2O_2 is efficient for the degradation of organic pollutants, i.e., aniline, phenolic compounds, and other aromatic compounds [11,12].

Despite its feasibility, enzymatic degradation is limited for practical application in the degradation of organic pollutants due to the difficulty of enzyme recovery and the requirement for a continuous external supply of H_2O_2. To overcome these limitations, Lee et al. [13] proposed the electroenzymatic process that combined enzymatic catalysis and the electrochemical reaction to carry out the degradation of 2,4,6-trinitrotoluene (TNT) using *in-situ* generated H_2O_2 within an electrochemical reactor containing immobilized HRP.

In an electroenzymatic process, electrogenerated H_2O_2 plays an important role in the activation of peroxidases that result in the degradation of organic pollutants. As such, the accurate measurement of the electrogenerated H_2O_2 is useful in the comprehension of this overall process. To date, various chemical methods have been used for the determination of H_2O_2 using metallic compounds such as titanium oxalate, titanium tetrachloride [14–17] and cobalt (II) ion [18] that form colored complexes with H_2O_2 that can then be spectrometrically measured. These methods, however, cannot apply real-time detection of the generated H_2O_2 within the electrochemical reactor.

Microelectrodes for the measurement of H_2O_2 have been developed using cellulose acetate [19], mesoporous platinum [20], and carbon fiber [21]. Among them, carbon fiber is the most attractive material since it is very cheap, well-studied, and has a favorable surface structure. To this end, Wang et al. [22] studied the determination of H_2O_2 by using a polyaniline (PAn) film and platinum particles co-modified carbon fiber microelectrode. They reported that the carbon fiber microelectrode had a high response to H_2O_2 with low noise and instability.

* Corresponding author. Tel.: +82 62 970 2435; fax: +82 62 970 2434.
E-mail address: shmoon@gist.ac.kr (S.-H. Moon).

0304-3894/$ – see front matter © 2009 Elsevier B.V. All rights reserved.
doi:10.1016/j.jhazmat.2009.09.157

In this study, the kinetics of the electrogenerated H_2O_2 in the electrochemical reactor was examined using a carbon fiber microelectrode modified with a PAn film and platinum particles. In addition, degradation kinetics of the phenol via an electroenzymatic process was amperometrically determined by the current response of the carbon fiber microelectrode.

2. Experimental

2.1. Materials

To construct the microelectrode for the measurement of H_2O_2, carbon fiber (0.8 μm diameter, 60 mm length, Johnson and Matthey Corp., USA), K_2PtCl_6 (Sigma–Aldrich, USA) and polyaniline (Sigma–Aldrich) were used.

HRP (type VI-A, EC 1.11.1.7, Sigma, USA) immobilization was performed using 1-ethyl-3-(3-dimethylaminopropyl)carbodiimide hydrochloride (EDC, Sigma–Aldrich, USA) and *N*-hydroxysuccinimide (NHS, Aldrich, USA) on reticulated vitreous carbon (RVC, 100 ppi (pores per linear inch), Duocel, ERG Materials and Aerospace Corp., USA). Other chemicals used in this study were obtained from Sigma–Aldrich Chemical Company (USA) and all solutions were prepared with double deionized water.

2.2. Preparation of carbon fiber microelectrode and electrochemical instrument

To enhance the sensitivity and stability of the carbon fiber microelectrode, conducting polyaniline (PAn) and platinum particles were used as described in a previous study [22]. The washed carbon fiber in a mixture solution of acetone and nitric acid (1:1, v/v) was inserted into the glass capillary and its tip was sealed by epoxy resin that is a mixture of weld agent and hardening agent (Permatex # 14600 series). The carbon fiber microelectrode was coated using 150 mL of 0.1 M aniline in 1.0 M H_2SO_4 between −0.2 and +0.9 V at 100 mV s^{-1} for 20 cycles under well mixed condition. The PAn-coated microelectrode was platinized using 2.0×10^{-3} M K_2PtCl_6 in 0.5 M H_2SO_4 at −0.2 V for 10 min; further coating of another layer of PAn film was performed in the same manner. For platinization and PAn-coating of the carbon microelectrode, a PGSTAT30/GPES system (Eco Chemie, Netherlands) was used.

Also, for the amperometric detection of H_2O_2, a three-electrode cell was used. This cell was equipped with the prepared carbon fiber microelectrode, a platinum wire and Ag/AgCl (in 3.3 M KCl) as the working electrode, counter electrode and reference electrode, respectively. Chronoamperometry was carried out using a PGSTAT 30 controlled by GPES software.

2.3. Immobilization of HRP on the RVC surface

For the immobilization of HRP, RVC possessing high surface area and good electric property was chosen. The immobilization procedures followed those of Williams et al. [23] which described the attachment of DNA to carbon nanotubes. The RVC was treated in a 3:1 mixture of concentrated H_2SO_4 and HNO_3 for 1 h. To produce abundant carboxyl end-groups, the treated RVC was exposed to 1.0 M HCl. Then this RVC was dispersed in dimethylformamide (DMF) and incubated in EDC and 5 mM NHS at 4 °C. After addition of 1000 U ml^{-1} HRP, this RVC was reacted in DMF.

2.4. Electrochemical reactor immobilized HRP and electrochemical instrument

A two-compartment electrochemical reactor (effective volume of each compartment: 150 mL) was used and a proton exchange membrane (Nafion 117, DuPont, USA) was placed between two compartments as shown in Fig. 1. The Pt coated on the Ti plate (Pt/Ti) and the RVC immobilized HRP (HRP/RVC) were used as anode and cathode, respectively. The anolyte was 100 mM phosphate buffer solution (PBS), and a certain amount of phenol dissolved in 100 mM PBS was used as the catholyte. The potential between the anode and cathode was applied using a DC power supply (6613C, Agilent, USA).

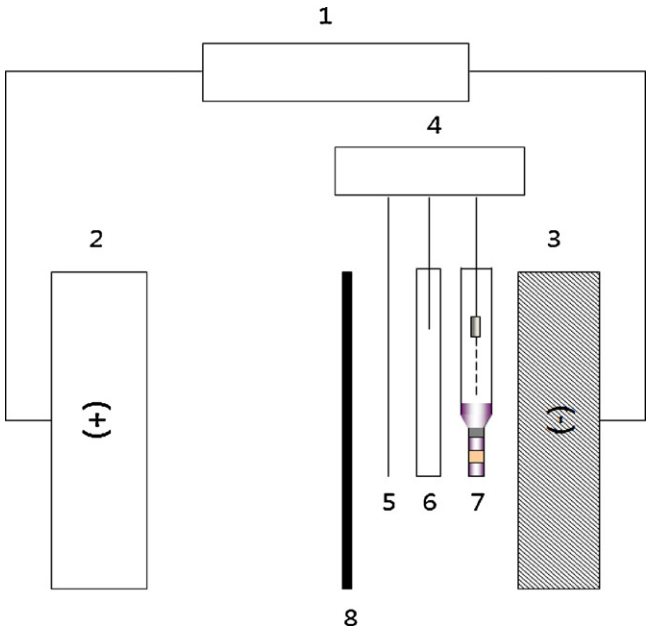

Fig. 1. Schematic diagram of the electrochemical reactor immobilized HRP on RVC and electrochemical instrument. (1) DC power supply, (2) anode (Pt/Ti), (3) cathode (HRP/RVC), (4) potentiostat, (5) counter electrode (Pt wire), (6) reference electrode (Ag/AgCl), (7) working electrode (carbon fiber microelectrode), (8) proton exchange membrane (Nafion 117).

2.5. Analysis

To compare with amperometric measurement of H_2O_2, the DMP method was performed by using copper (II) ion and 2,9-dimethyl-1,10-phenanthroline (DMP) at 453 nm in UV–vis spectroscopy (Simatzu, Japan) [24]. The concentration of phenol was determined at 270 nm through the use of a UV–vis spectrophotometer after filtration (45 μm, Millipore, USA).

3. Results and discussion

3.1. Preparation of microelectrode for detection of the electrogenerated H_2O_2

Fig. 2 shows the current response of a carbon fiber microelectrode to the amount of H_2O_2 at −0.6 V (vs. Ag/AgCl). As can be seen, the current signal linearly increased with the amount of H_2O_2 since the responding current was diffusion-limited; this linear equation can be expressed as followed equation

$$i[\mu A] = 2.19 C_{H_2O_2}[mM] - 0.044 \quad (1)$$

Here, the microelectrode enabled the fast measurements due to the high conductivity of the coated PAn film and platinum particles at the end of the carbon fiber microelectrode. The time to reach a steady state increased from 10 s to 14 s when the concentration of H_2O_2 increased, in agreement with the Cottrell equation that describes the current with respect to time in a controlled potential [25].

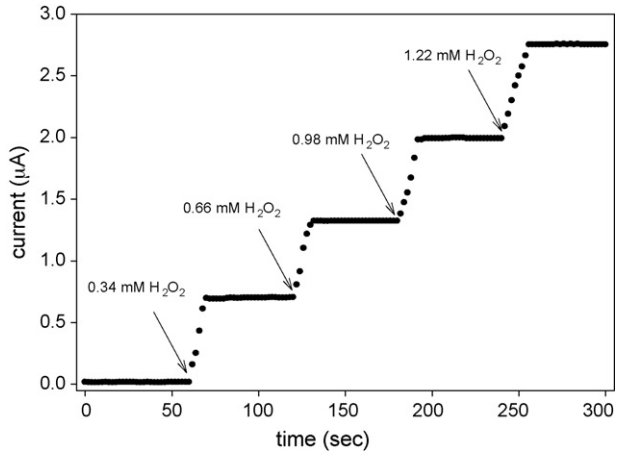

Fig. 2. Current response of the carbon fiber microelectrode to the external addition of H_2O_2 at −0.6 V (vs. Ag/AgCl). Working electrode (WE): carbon fiber microelectrode; counter electrode (CE): Pt wire; reference electrode (RE): Ag/AgCl in 3.3 M KCl solution.

3.2. Measurement of the electrogenerated H_2O_2 using a carbon fiber microelectrode

For the real-time measurement of electrogenerated H_2O_2, a three-electrode system including a carbon fiber microelectrode as the working electrode was set in an electrochemical reactor equipped with a Pt/Ti anode and a reticulated vitreous carbon (RVC) cathode. Fig. 3 compares the current response of the carbon fiber microelectrode inside the electrochemical reactor with that outside the electrochemical reactor when 2.3 V is applied at pH 7.0. In both cases, the increasing rate of current responses was similar at 0.018 μA min^{-1} since the electrogenerated H_2O_2 was accumulated within the electrochemical reactor prior to the response of the current for the H_2O_2. Also, the initial current response directly measured inside the electrochemical reactor was 0.55 μA higher than that indirectly measured outside the electrochemical reactor since it was influenced by the electric field.

3.2.1. Effect of electrolyte pH

Fig. 4 presents the current responses for the measurement of the electrogenerated H_2O_2 with various electrolyte pHs that were adjusted using 100 mM PBS in the range of pH 5.0–9.0. It was observed that in the weakly acidic and neutral conditions, slopes were above 0.0180 μA min^{-1} whereas the slopes were 0.0136 μA min^{-1} and 0.0107 μA min^{-1} for pH 8.0 and pH 9.0, respectively. The difference implies that the electrogenerated H_2O_2 was dependent on the pH, and that the weakly acidic condition, especially pH 6.0, was more suitable for the electrogeneration of H_2O_2 than the weakly basic conditions.

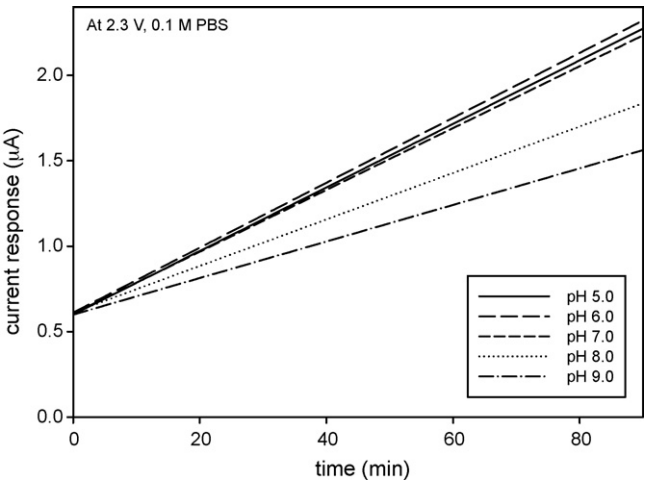

Fig. 4. Current response of a carbon fiber microelectrode to electrogenerated H_2O_2 at −0.6 V (vs. Ag/AgCl) inside the electrochemical reactor as a function of electrolyte pH. Data measurement: 1 point/25 s; applied potential: 2.3 V (anode-Pt/Ti, cathode-RVC); electrolyte: 0.1 M PBS.

3.2.2. Effect of applied potential

The effect of applied potential was also examined in terms of power density and the slope of current response, as shown in Fig. 5. For voltages below 2.3 V, the power density slightly increased from 4.9 W m^{-2} to 21.1 W m^{-2} due to the Ohmic resistance. Above 2.3 V, however, the power density steeply increased to 95.2 W m^{-2} since a charge transfer resistance was caused by the excess protons (H^+) and hydroxide ions (OH^-) generated from water dissociation [26].

In the range of 1.3–2.3 V, the slope of the current response increased from 0.0113 μA min^{-1} to 0.0190 μA min^{-1} according to the applied potential. This increase implies that the required electrical energy for the reduction of oxygen to H_2O_2 via the two-electron reaction, $O_2 + 2H^+ + 2e^- \rightarrow H_2O_2$, was fully supplied

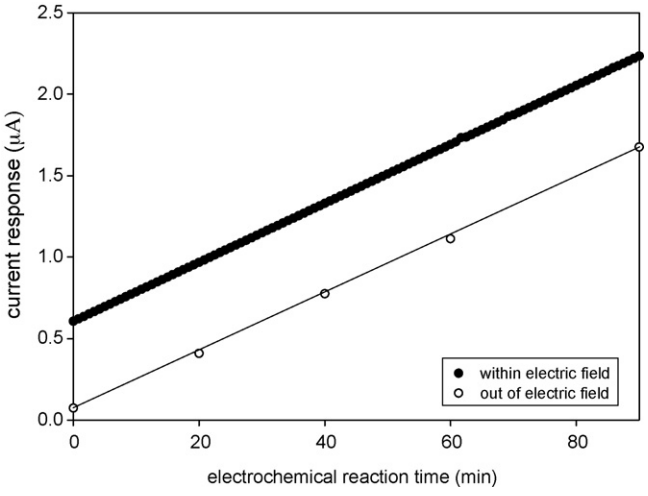

Fig. 3. Current response of a carbon fiber microelectrode to electrogenerated H_2O_2 at −0.6 V (vs. Ag/AgCl): (●) inside the electrochemical reactor and (○) outside the electrochemical reactor. Applied potential: 2.3 V (anode-Pt/Ti, cathode-RVC), electrolyte: 0.1 M PBS (pH 7.0).

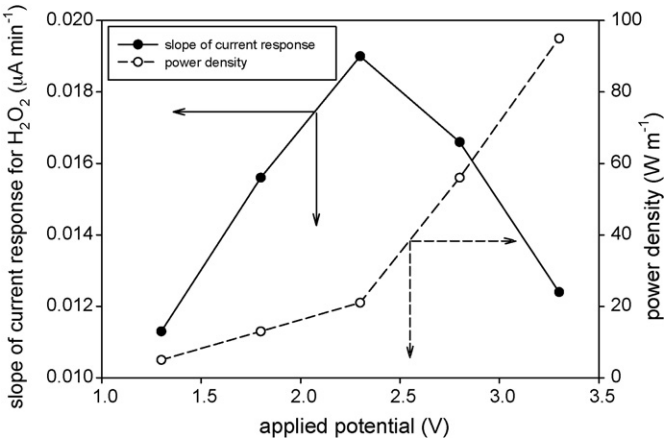

Fig. 5. Production characteristics of H_2O_2 within the electrochemical reactor as a function of the applied potential between Pt/Ti anode and RVC cathode. (●) Increasing rate of current response for H_2O_2 and (○) power density.

at 2.3 V, whereas it was insufficient at a lower voltage. Above 2.8 V, however, it decreased to 0.0124 μA min^{-1} since the oxygen was converted to water molecules via the four-electron reaction, $O_2 + 4H^+ + 4e^- \rightarrow 2H_2O$, when a potential greater than the required electrical energy for H_2O_2 generation was applied. Therefore, it was considered that the optimal applied potential was 2.3 V, at which a two-electron reaction takes place, predominantly by water dissociation.

3.2.3. Stability of carbon fiber microelectrode

Based on the change of the slope of current response for H_2O_2, the stability of a carbon fiber microelectrode was then examined. A relative ratio of current response was 0.98 to the initial slope during continuous 11 assays of carbon fiber microelectrode at 2.3 V between the Pt/Ti and RVC electrodes in 0.1 M PBS at pH 6.0. Also, the current response of the carbon fiber microelectrode was maintained beyond 11 assays, although it slightly decreased to 0.95 of the relative ratio compared to the initial value. The slight decrease suggests that there was no severe damage of the carbon fiber microelectrode for the electron transfer mechanism through the conducting PAn film and platinum particles.

3.3. Degradation kinetics of phenol using an electroenzymatic process

Fig. 6 illustrates the difference in current responses in the absence of phenol with that in the presence of phenol as substrate. The electrogenerated H_2O_2 was consumed during enzymatic degradation in the presence of phenol though it remained without consumption in the absence of phenol. As shown in the figure, the difference in current response linearly increased since H_2O_2 was continuously generated in the absence of phenol whereas it was completely consumed in the presence of phenol during the enzymatic degradation of phenol. A plateau was formed when the phenol was completely degraded at 12.50 min, 22.50 min and 43.33 min for 0.1 mM, 0.2 mM and 0.4 mM of phenol, respectively. The time differences imply that more H_2O_2 was required to degrade more phenol, and that the generation rates of the electrogenerated H_2O_2 in the presence of phenol was the same as that in the absence of phenol when the electroenzymatic degradation of phenol was completed. The average rate constant of phenol degradation was 1.45×10^{-7} mol L^{-1} s^{-1} through electroenzymatic reaction when Fe (III) in HRP was oxidized to Fe (IV) by electrogenerated H_2O_2 [27].

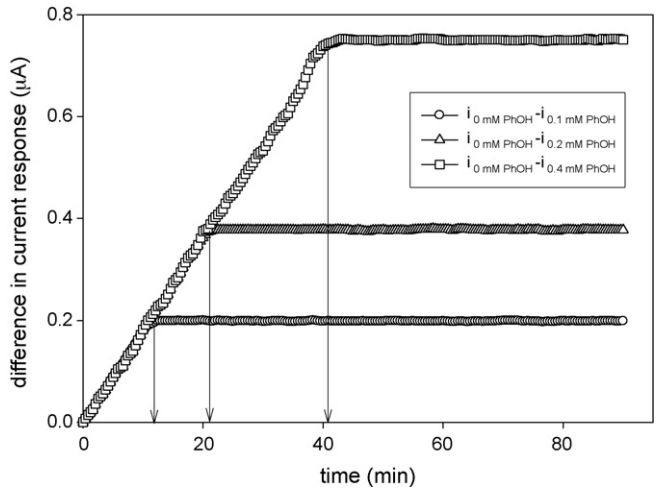

Fig. 6. Difference in current response between absence and presence of phenol in the concentration rage of 0.1–0.4 mM. Data measurement: 1 point/25 s; applied potential: 2.3 V (anode-Pt/Ti, cathode-RVC); electrolyte: 0.1 M PBS (pH 6.0).

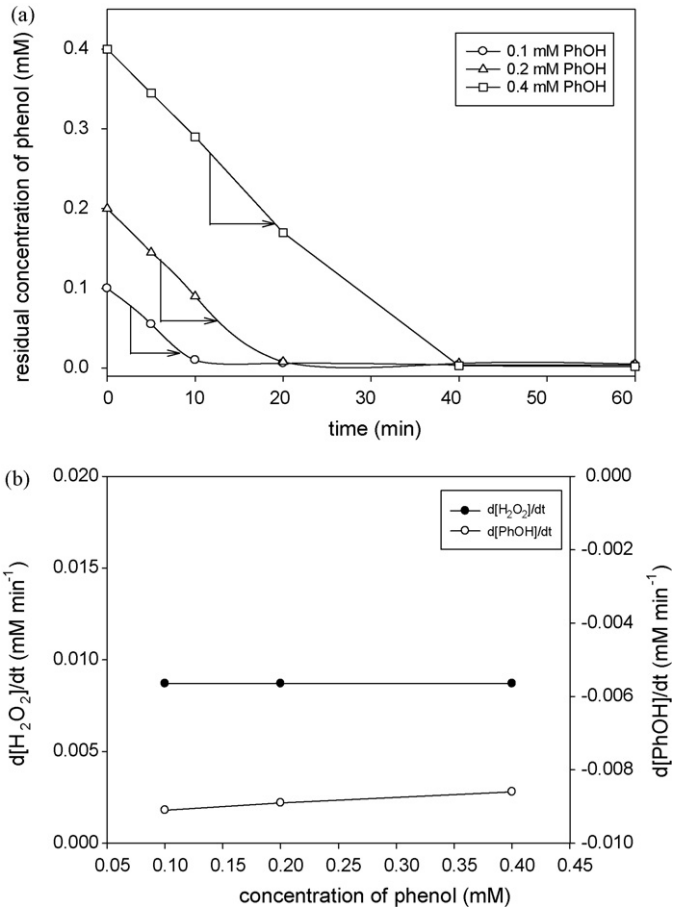

Fig. 7. (a) Change of residual concentration of phenol according to the electrochemical reaction time for (○) 0.1 mM phenol, (△) 0.2 mM phenol, and (□) 0.4 mM phenol. Applied potential: 2.3 V (anode-Pt/Ti, cathode-RVC); electrolyte: 0.1 M PBS (pH 6.0); (b) (●) the electrogeneration rate of H_2O_2 and (○) the electroenzymatic degradation rate of phenol.

3.4. Estimation of kinetics in electroenzymatic degradation of phenol

Fig. 7(a) shows the change of residual concentration of phenol in the determination of the degradation rate in the electrochemical reactor immobilized HRP as a function of phenol concentration. As can be seen in the figure, the residual concentration of phenol decreased linearly with the electrochemical reaction time until the degradation of phenol was completed. This suggests that H_2O_2 was continuously electrogenerated and played a role in the degradation of phenol. The degradation rates could then be determined by the ratio of phenol decrease to the time for complete degradation.

The electroenzymatic degradation rate of phenol is shown in Fig 7(b) with the various production rate of the electrogenerated H_2O_2. Phenol was degraded at a rate of 0.0091–0.0086 mM min^{-1} in the range of 0.1–0.4 mM of the feed concentration. The H_2O_2 was electrogenerated at a rate of 0.0087 mM min^{-1} and was independent of the concentration of phenol. Therefore, the stoichiometric ratios between phenol and the electrogenerated H_2O_2 were 1.04:1, 1.02:1 and 0.99:1; the concentration of phenol being similar to previous results [28], where the apparent stoichiometric ratio was determined as 1:1, between phenol and the externally added H_2O_2 in the presence of aqueous HRP. Therefore, the phenol could be completely degraded by the electroenzymatic method under certain stoichiometric ratios between electrogenerated H_2O_2 and phenol.

4. Conclusion

The kinetics of electrogenerated H_2O_2 was determined using a carbon fiber microelectrode that was modified by polyaniline film and platinum particles. The generation rate of H_2O_2 was found to vary as an effect of pH and the applied potential, and led to variance in the current response of a carbon fiber microelectrode. The electrogenerated H_2O_2 formed at a rate of $0.0190\,\mu A\,min^{-1}$ when 2.3 V was applied between a Pt/Ti anode and an RVC cathode at pH 6.0. Aqueous phenol was completely degraded using the electroenzymatic process and the stoichiometric ratio between the electrogenerated H_2O_2 and the optimum degradation of aqueous phenol under HRP immobilized on RVC was confirmed to be 1:1.

Acknowledgement

This work was supported by the Research Center for Biomolecular Nanotechnology at Gwangju Institute of Science and Technology (GIST).

References

[1] J.M.C. Martin, G.B. Brieva, J.L.G. Fierro, Hydrogen peroxide synthesis: an outlook beyond the anthraquinone process, Angew. Chem. Int. Ed. 45 (2006) 6962–6984.
[2] F. Alcaide, P.L. Cabot, E. Brillas, Fuel cells for chemicals and energy cogeneration, J. Power Sources 153 (2006) 47–60.
[3] F.J. Rivas, S.T. Kolaczkowski, F.J. Beltran, D.B. McLurgh, Hydrogen peroxide promoted wet air oxidation of phenol: influence of operating conditions and homogeneous metal catalysts, J. Chem. Technol. Biotechnol. 74 (1999) 390–398.
[4] F. López, M.J. Díaz, M.E. Eugenio, J. Ariza, A. Rodríguez, L. Jiménez, Optimization of hydrogen peroxide in totally chlorine free bleaching of cellulose pulp from olive tree residues, Bioresour. Technol. 87 (2003) 255–261.
[5] M.F. Sevimil, Post-treatment of pulp and paper industry wastewater by advanced oxidation processes, Ozone Sci. Eng. 27 (2005) 37–43.
[6] F.J. Benitez, J.L. Acero, T. Gonzalez, J. Garcia, Organic matter removal from wastewaters of the black olive industry by chemical and biological procedures, Process Biochem. 37 (2001) 257–265.
[7] A. Couvert, I. Charron, A. Laplanche, C. Renner, L. Patria, B. Requieme, Treatment of odorous sulphur compounds by chemical scrubbing with hydrogen peroxide—application to a laboratory plant, Chem. Eng. Sci. 61 (2006) 7240–7248.
[8] M. Pérez, F. Torrades, X. Domènech, J. Peral, Fenton and photo-Fenton oxidation of textile effluents, Water Res. 36 (2002) 2703–2710.
[9] H.B. Dunford, J.S. Stillman, On the function and mechanism of action of peroxidases, Coord. Chem. Rev. 19 (1976) 187–251.
[10] P.J. Kerstern, M. Tien, B. Kalyanaraman, T.K. Kirk, The ligninase of *Phanerochaete chrysosporium* generates cations radicals from methoxybenzenes, J. Biol. Chem. 260 (1985) 2609–2612.
[11] A.M. Klibanov, Enzymatic removal of toxic phenols and anilines from wastewaters, J. Appl. Biochem. 2 (1980) 414–421.
[12] V.S. Ferreira-Leitão, M.E.A. de Carvalho, E.P.S. Bon, Lignin peroxidase efficiency for methylene blue decolouration: comparison to reported methods, Dyes Pigm. 74 (2007) 230–236.
[13] K.B. Lee, M.B. Gu, S.H. Moon, In-situ generation of hydrogen peroxide and its use for enzymatic degradation of 2,4,6-trinitrotoluene, J. Chem. Technol. Biotechnol. 76 (2001) 811–819.
[14] M. Sunder, D.C. Hempel, Oxidation of tri- and perchloroethene in aqueous solution with ozone and hydrogen peroxide in a tube reactor, Water Res. 31 (1997) 33–40.
[15] N. Karpel Vel Leitner, M. Doré, Mechanism of the reaction between hydroxyl radicals and glycolic, glyoxylic, acetic and oxalic acids in aqueous solution: consequence on hydrogen peroxide consumption in the H_2O_2/UV and O_3/H_2O_2 systems, Water Res. 31 (1997) 1383–1397.
[16] C. Volk, P. Roche, C. Renner, H. Paillard, J.C. Joret, Effects of ozone-hydrogen peroxide combination on the formation of biodegradable dissolved organic carbon, Ozone Sci. Eng. 15 (1993) 405–418.
[17] P. Roche, M. Prados, Removal of pesticides by use of ozone or hydrogen peroxide/ozone, Ozone Sci. Eng. 17 (1995) 657–672.
[18] H. Gulyas, R. Von Bismarck, L. Hemmerling, Treatment of industrial wastewater with ozone/hydrogen peroxide, Water Sci. Technol. 32 (1995) 127–134.
[19] X. Liu, F. Roe, A. Jesaitis, Z. Lewandowski, Resistance of biofilms to the catalase inhibitor 3-amino-1, 2,4-triazole, Biotechnol. Bioeng. 59 (1998) 156–162.
[20] S.A.G. Evans, J.M. Elliott, L.M. Andrews, P.N. Bartlett, P.J. Doyle, G. Denuault, Detection of hydrogen peroxide at mesoporous platinum microelectrodes, Anal. Chem. 74 (2002) 1322–1326.
[21] E. Csőregl, L. Gorton, G. Marko-Varga, Peroxidase-modified carbon fiber microelectrodes in flow-through detection of hydrogen peroxide and organic peroxides, Anal. Chem. 66 (1994) 3604–3610.
[22] Y. Wang, J. Huang, C. Zhang, J. Wei, X. Zhou, Determination of hydrogen peroxide in rainwater by using a polyaniline film and particles co-modified carbon fiber microelectrode, Electroanal. 10 (1998) 776–778.
[23] K.A. Williams, P.T.M. Veenhuizen, B.G. de la Torre, R. Eritja, C. Dekker, Nanotechnology: carbon nanotubes with DNA recognition, Nature 420 (2002) 761.
[24] K. Kosaka, H. Yamada, S. Matsui, S. Echigo, K. Shishida, Comparison among the methods for hydrogen peroxide measurements to evaluate advanced oxidation processes: application of a spectrophotometric method using copper(II) ion and 2,9-dimethyl-1,10-phenanthriline, Environ. Sci. Technol. 32 (1998) 3821–3824.
[25] A.J. Bard, L.R. Faulkner, Electrochemical Methods: Fundamentals and Applications, 2nd edition, John Wiley & Sons, Inc., New York, 2000.
[26] S.H. Cho, J. Shim, S.H. Yun, S.H. Moon, Enzyme-catalyzed conversion of phenol by using immobilized horseradish peroxidase (HRP) in a membraneless electrochemical reactor, Appl. Catal. A 337 (2008) 66–72.
[27] P.K. Kersten, B. Kalyanaraman, K.E. Hammel, B. Reinhammer, T.K. Kirk, Comparison of lignin peroxidase, horseradish peroxidase and laccase in the oxidation of methoxybenzenes, Biochem. J. 268 (1990) 475–480.
[28] P.T. Vasudevan, L.O. Li, Peroxidase catalyzed polymerization of phenol, Appl. Biochem. Biotechnol. 60 (1996) 73–82.